Development of a High-Bandwidth Waveform Processing System using RFSoC for RI Beam Experiments

S. Takeshige*,†, H. Baba†, K. Kurita*, Y. Togano†, J. Zenihiro‡, and Y. Hijikata†,‡
*Department of Physics, Rikkyo University, 3-34-1 Nishi-Ikebukuro, Toshima-ku, 171-8501, Tokyo, Japan
†RIKEN Nishina Center for Accelerator-Based Science, 2-1 Hirosawa, Wako, 351-0198, Saitama, Japan
‡Department of Physics, Kyoto University, Kitashirakawa-Oiwake, Sakyo-ku, 606-8502, Kyoto, Japan
Email: stakeshige@rikkyo.ac.jp

***Abstract*—We have developed a digital waveform processing system with AMD RFSoC. It is the optimized system for experiments at RIKEN RI Beam Factory (RIBF) that is an accelerator facility in Japan. This system is aimed at simultaneous measurement of TOF with high-resolution and ΔE using plastic scintillators. The AMD RFSoC includes 4.096 GSPS ADC, FPGA, and CPU, and it is expected that a system that allows pipeline processing of high-frequency signals without dead time can be established. By adopting centroid calculation for the waveform processing method, a timing resolution of 9 ps in σ was achieved.**

***Index Terms*—RFSoC, Waveform processing systems, DAQ, TOF measuremnt, High-intensity beam, Radioactive ion beam**

I. Introduction

The RI Beam Factory (RIBF) [1], a rare isotope (RI) beam facility, has been in operation at the RIKEN Nishina Center since March 2007. A new generation of in-flight fragment separator, named BigRIPS [2]–[4], enables experimental studies using a wide variety of RI beams. The two-stage structure of BigRIPS [5] allows the delivery of tagged RI beams and excellent isotope separation. Particle identification is based on the TOF-$B\rho$-ΔE method. In this method, time-of-flight (TOF), magnetic rigidity ($B\rho$), and energy loss (ΔE) are measured to deduce the atomic number *(Z)* and mass-to-charge ratio *(A/Q)* of particles. We deduce the Z and *A/Q* values from the measured TOF, $B\rho$, and ΔE using the equations as follows:

$$TOF = \frac{L}{\beta c}, \tag{1}$$

$$\frac{A}{Q} = \frac{B\rho}{\beta\gamma}\frac{c}{m_u}, \tag{2}$$

$$\frac{\Delta E}{dx} = \frac{4\pi e^4 Z^2}{m_e v^2} N z [\ln\frac{2m_e v^2}{I} - \ln(1-\beta^2) - \beta^2], \tag{3}$$

where L is the flight path length, v ($\beta = v/c; \gamma = 1/\sqrt{1-\beta^2}$, c is the speed of light) is the particle velocity, m_u =931.494 MeV is the atomic mass unit, m_e is the electron mass, and e is the elementary charge. z, N, and I represent the atomic number, atomic density, and average excitation potential of the material, respectively; Z, A, and Q represent the atomic number, mass number, and charge (or charge state) number of the particle, respectively. The Bethe-Bloch equation [6], [7] shown in Equation 3 describes the energy loss ΔE.

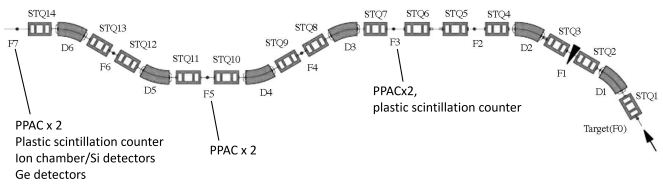

Fig. 1. Schematic layout of the BigRIPS separator.

Fig. 1 shows the schematic layout of the BigRIPS separator and the typical setup of the beam-line detector used for particle identification of RI beams. As shown in Fig. 1, TOF is measured using thin plastic scintillation counters located at F3 and F7, at the beginning and end of the second stage of the BigRIPS separator, respectively; ΔE is measured using a multi-sampling ionization box (MUSIC) [8] detector located at F7 $B\rho$ is measured by trajectory reconstruction [9]–[11] in the first half of the second stage (F3–F5) as well as in the second half (F5–F7), as shown in Fig. 1. For trajectory reconstruction, the position and angle of the particles are measured using two sets of position-sensitive parallel plate avalanche counters (PPACs) [12] placed at each focus. Ion optical transfer matrix elements up to third order, estimated from experimental data, are used for trajectory reconstruction.

A timing resolution of TOF σ 40 ps is required for particle identification [13]. To achieve this timing resolution, walk correction is performed using charge information from a charge ADC in addition to time information from a TDC. Conventional ADCs and TDCs of CAMAC and VME standards used in RIBF have a long dead time and have become a bottleneck in measurement. RIKEN RIBF is planning to upgrade its data acquisition system to handle higher beam intensities with a trigger rate of 100 kHz or higher. In recent DAQ, for example, for Ge semiconductor detectors, instead of CAMAC or VME standard ADC or TDC, a digitizer

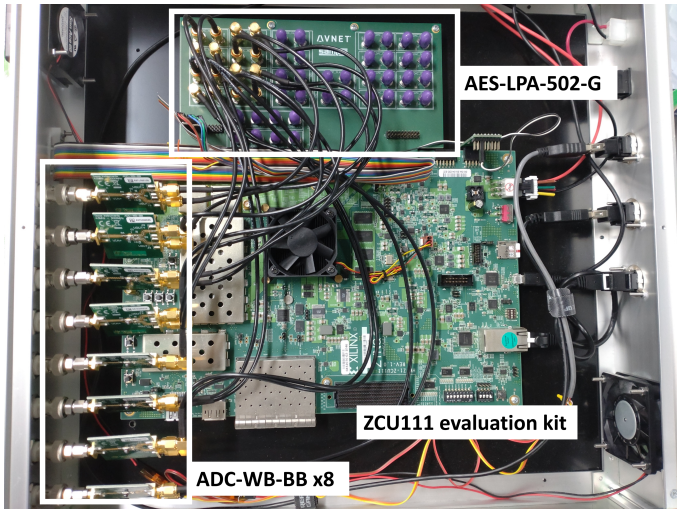

Fig. 2. Photograph of ZCU111 evaluation kit with the AES-LPA-502-G and the ADC-WB-BB.

is used to acquire signal waveforms and perform real-time waveform processing. This allows measurement systems with short processing times. The sampling rate of these digitizers is generally 100 to 500 MHz, which is not suitable for acquiring signals from plastic scintillators. With this background, we attempt to achieve real-time waveform processing of plastic scintillators to obtain excellent time resolution by combining a digitizer with a GHz sampling rate and an FPGA. In this paper, we describe the method of extracting time information by centroid calculation, the results of off-line analysis, and the algorithm of real-time centroid calculation.

II. Device

The RFSoC [14] is a system developed for 5G communications, and part number XCZU28DR- 2FFVG1517E has 8 channels 12 bit 4.096 GSPS ADC, 14 bit 6.554 GSPS DAC, FPGA, and CPU in a single chip. The analog bandwidth is 4 GHz. The RFSoC device is capable of performing AD conversion, digital signal processing, and network data transfer required for a DAQ system on a single chip. The AMD ZCU111 evaluation kit [15] and the differential breakout card AES-LPA-502-G [16] from AVNET ware used for system development. The ADC of the RFSoC device has a 100 Ω differential input. TEXAS INSTRUMENTS wideband balun board ADC-WB-BB [17] with a frequency range of 4.5–3000 MHz is used to convert a 50 Ω single-ended signal to a 100 Ω terminated differential signal.

III. Waveform processing method

The leading-edge method is commonly used to obtain time information from plastic scintillators. This method provides time information on when the signal height exceeds the threshold voltage. To obtain high timing resolution with the leading edge method, it is important to minimize noise. The timing jitter of the leading edge method depends on the $\sigma v/\frac{dV}{dt}$ of the signal, where σn is the signal noise and $\frac{dV}{dt}$ is the slope of the signal at the point where the threshold is exceeded. Thus a detector signal with a fast rise time will achieve good time resolution. The leading edge method is not appropriate for obtaining time information from waveforms acquired using a digitizer. Since timing jitter is determined by the sampling rate e.g., sampling rate with 4 GHz gives 72.2 ps rms timing resolution. Therefore, waveform processing is necessary.

There are some methods to obtain time information by waveform analysis, such as obtaining the zero-crossing point from the waveform after differentiation, and the intersection of the baseline and the linear extrapolation of the rising slope. However, the function of the rising slope of the waveform includes various factors such as the scintillation mechanism, size, and shape of a detector, response of photo sensors, and bandwidth of the transmission path, thus, a simple linear extrapolation of the rising slope does not always provide good timing. The centroid calculation method is studied to obtain time information by waveform processing. The centroid calculation method can obtain stable results that are not affected by the function of the rising slope of the signal.

The centroid of the waveform G was expressed by the following equation

$$G = \frac{\sum(v_i \times i)}{\sum v_i}, \tag{4}$$

where v_i is the i-th data of the acquired waveform. In the centroid calculation method, it is also important to eliminate noises from signals as much as possible. Considering error propagation for the numerator in eq. 4, the error dg is described by eq. 5 The numerator is greatly affected by noise because the error is weighted by the clock number.

$$dg = \sqrt{\sum(\frac{\partial g}{\partial v_i}dv_i)^2} = \sqrt{\sum(i \times dv_i)^2}, \tag{5}$$

In this system, noise elimination is performed in two stages: smoothing and limiting the calculation range. All acquired signals are smoothed by taking a moving average.

$$A_i = \frac{x_i + x_{i-1} + ... + x_{i-(n-1)}}{n} \tag{6}$$

Fig. 3 shows the difference in frequency response depending on the number of smoothing points. From Fig. 3, noise components above 100 MHz could be suppressed by setting the appropriate number of smoothing points. On the other hand, it is difficult to exclude low-frequency noise. To minimize the effects of low-frequency noise, the calculation range is limited.

The overview of waveform processing is shown in Fig. 4 First, the signal sent from the detector is smoothed. The smoothed signal is distributed into two signals. One of the signals is accumulated in a shift register for centroid calculation. The other signal is used to search for a peak position. The peak position is obtained by differentiating the acquired signal. Set a threshold on the waveform after differentiation and search for the zero crossing point of the signal after the threshold is exceeded. The zero crossing point corresponds to the peak position. The centroid calculation is started after the peak position is detected.

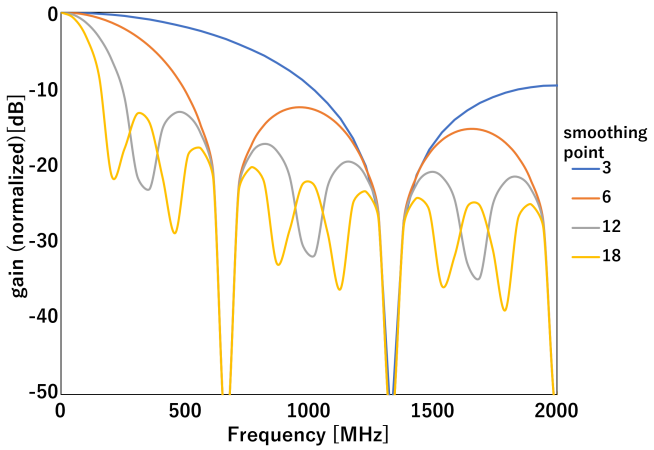

Fig. 3. The difference in frequency response at 4.096 GSPS depending on the number of smoothing points.

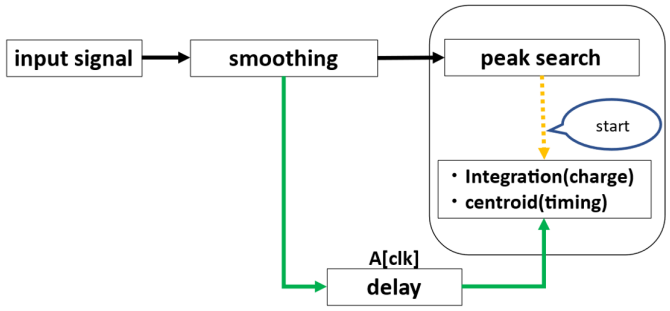

Fig. 4. The overview of waveform processing.

IV. Result

To verify whether the time resolution obtained by centroid calculations meets the requirement of better than 40 ps in σ, waveform data were acquired by ZCU111, and centroid calculations were performed by offline analysis. The circuit diagram which the waveform was obtained is shown in Fig. 5. A pulse that simulated a plastic scintillator signal was used. The pulse is distributed using a Linear Fan in Fan out. One of the pulses was converted to a logic signal using a discriminator and input to ZCU111 as an external trigger. The two signals were also input to channel-0 and channel-1 of the ZCU111. The waveforms of the input pulses were acquired, then smoothing and centroid calculations were performed, and the time difference between the two channels was calculated. A moving average of 9 points was applied as smoothing. The centroid calculation was performed using the data points from -60 clocks to +70 clocks with respect to the detected peak position. The result is shown in Fig. 6. By applying centroid calculations, a result of σ = 9 ps was obtained. The resolution was sufficiently high for the TOF measurement in RIBF experiments.

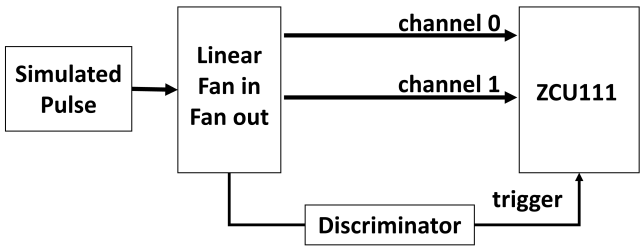

Fig. 5. The circuit diagram which the waveform was obtained to verify timing resolution in centroid calculations.

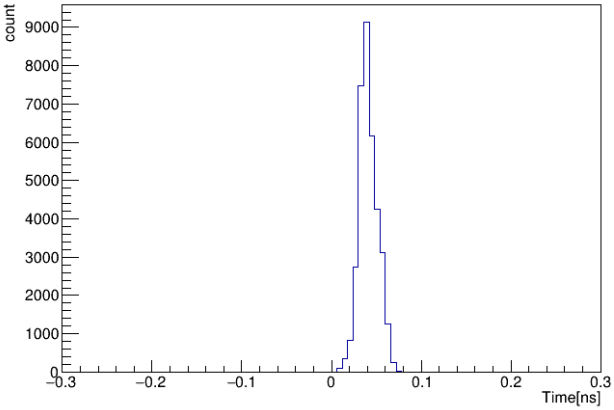

Fig. 6. The time difference between the two channels of ZCU111 obtained by smoothing and centroid calculations.

V. Summery

A real-time digital waveform processing system using RFSoC devices is under development. We confirmed the centroid calculation is a suitable method of acquiring time information. There is an issue in implementing the developed algorithm to RFSoC. The sampling rate of ADC-block installed in the RFSoC is 4.096 GSPS. On the other hand, the internal clock frequency of the FPGA-block is 512 MHz. 8 data points of the waveform are packed and sent to the FPGA-block every 1 clock. To process data in an RFSoC device, it is necessary to process 8 data points sent together at 512 MHz clock. There are two possible methods: The 8 data points are divided into cases according to the calculation range and each data is calculated simultaneously, or they are divided into multiple FIFOs and stored in time, and serial calculations are performed in parallel. The implementation of centroid calculation in programmable logic is currently being studied.

References

[1] Toshiyuki Kubo, Nucl. Instr. Meth. B 204 (2003) 97.
[2] Yasushige Yano, "The RIKEN RI Beam Factory Project: A status report" Nucl. Instr. Meth. B 261 (2007) 1009.

[3] S. Nishimura, et al., "RIKEN RI Beam Factory," Nucl. Instrum. Methods Phys. Res. Sect. B, vol. 376, pp. 237-240, 2016. K. Yoshida, et al., "Particle identification in the second stage of BigRIPS," Nucl. Instrum. Methods Phys. Res. Sect. A, vol. 642, pp. 310-315, 2011.
[4] S. Takeuchi, et al., "Performance of BigRIPS fragment separator," Nucl. Instrum. Methods Phys. Res. Sect. A, vol. 593, pp. 134-142, 2008.
[5] Toshiyuki Kubo, Daisuke Kameda, Hiroshi Suzuki, Naoki Fukuda, Hiroyuki Takeda, Yoshiyuki Yanagisawa, Masao Ohtake, Kensuke Kusaka, Koichi Yoshida, Naohito Inabe, Tetsuya Ohnishi, Atsushi Yoshida, Kanenobu Tanaka, and Yutaka Mizoi, "BigRIPS separator and ZeroDegree Spectrometer at RIKEN RI Beam Factory," Prog. Theor. Exp. Phys., vol. 2012, no. 1, 03C003, 2012.
[6] H. Bethe, "Quantenmechanik der Ein- und Zwei-Elektronenprobleme", Handb. Phys. 24 (1933) 273.
[7] H. Bethe, "Bremsformel für Elektronen relativistischer Geschwindigkeit", Z. Phys. 76 (1932) 293.
[8] K. Kimura, T. Izumikawa, R. Koyama, T. Ohnishi, T. Ohtsubo, A. Ozawa, W.Shinozaki, T. Suzuki, M. Takahashi, I. Tanihata, T. Yamaguchi, Y. Yamaguchi, "High-rate particle identification of high-energy heavy ions using a tilted electrode gas ionization chamber", Nucl. Instr. Meth. A 538 (2005) 608.
[9] S. Takeuchi, et al., "Trajectory reconstruction method for particle identification," Nucl. Instrum. Methods Phys. Res. Sect. A, vol. 642, pp. 261-267, 2011.
[10] K. Yoshida, et al., "Particle trajectory reconstruction in BigRIPS," Nucl. Instrum. Methods Phys. Res. Sect. A, vol. 590, pp. 204-213, 2008.
[11] H. Kumagai, et al., "Position-sensitive parallel plate avalanche counters for BigRIPS separator," Nucl. Instrum. Methods Phys. Res. Sect. A, vol. 560, pp. 621-631, 2006.
[12] S. Takeuchi, et al., "Parallel plate avalanche counters for particle identification at BigRIPS," Nucl. Instrum. Methods Phys. Res. Sect. A, vol. 540, pp. 519-529, 2005.
[13] N. Fukuda, T. kubo,T. Ohnishi, N. Inabe, H. Takeda, D. Kameda, H. Suzuki, Nucl. Instr. Meth. B 317 (2013) 323-332.
[14] AMD, Zynq UltraScale+ RFSoC [Online]. Available: https://japan.xilinx.com/products/silicon-devices/soc/rfsoc.html
[15] AMD, Zynq UltraScale+ RFSoC ZCU111 Evaluation Kit, [Online]. Available: https://www.xilinx.com/products/boards-and-kits/zcu111.html
[16] AVNET, Samtec differential breakout card for ZYNQ Ultrascale+ RFSoC [Online]. Available: https://my.avnet.com/abacus/manufacturers/m/samtec/products/differential-breakout-card-for-zynq-ultrascale-rfsoc/
[17] Available: TEXAS INSTRUMENTS, ADC-WB-BB / ADC-LD-BB User's Guide, [Online]. https://www.tij.co.jp/jp/lit/ug/snau123/snau123.pdf